

## 2-3-3 Prediction System of the 1-AU Arrival Times of CME-Associated Interplanetary Shocks Using Three-Dimensional Simulations

DEN Mitsue, OGAWA Tomoya, TANAKA Takashi, WATARI Shinichi,  
AMO Hiroyoshi, SUGIHARA Kouta, and TAKEI Toshifumi

We describe prediction system of the 1-AU arrival times of interplanetary shock waves associated with coronal mass ejections (CMEs). The system is based on the modeling of shock propagation by using a three-dimensional adaptive mesh refinement (AMR) code. Once a CME is observed by LASCO/SOHO, the ambient solar wind is first obtained through numerical simulation, which reproduces the solar wind parameters at that time as observed by the ACE space-craft. Next we input data on the expansion velocity and position of where the CME occurred as initial conditions for a CME model, and then perform 3D simulations of the CME and shock propagation until the shock wave passes the 1-AU point. A Web interface is available for inputting the parameters, executing simulations, and outputting the results, so that even someone unfamiliar with computer operations or simulations, or who is not a researcher can use this system to predict the shock passage time. Simulated CME and shock evolution are visualized at the same time as the simulation, with related snapshots appearing automatically on the Web, so that user can follow the propagation. This system is expected to be useful for space weather forecasters. This paper describes the system and simulation model in detail.

### Keywords

Space weather simulator, Interplanetary shock wave, Three-dimensional numerical simulation

### 1 Introduction

It is known that CMEs, one of the solar phenomena, exert an immense effect on the upper atmosphere of the earth and space environments near the earth, through geomagnetic storms, ionospheric storms, and solar energetic particles. Interplanetary shock waves form during CME propagation and are often accompanied by a trailing flux rope behind the shock waves (see **2-1-3** in this special issue). Interaction with an intense southward interplanetary magnetic field involved in this flux rope interacts with the magnetosphere to induce geomagnetic and ionospheric storms. These interplanetary

shock waves can also be a source of acceleration in forming solar energetic particles through shock acceleration, with the flux of solar energetic particles often peaking as the shock waves pass by. Therefore it is useful for predicting the occurrence of space environmental disturbances caused by CME events to obtain the information in advance about the time when interplanetary shock waves will arrive near the earth.

NICT has developed the world's first system to predict space environmental disturbances that utilizes numerical simulations based on physical laws by using a rapidly developing supercomputer<sup>[1]</sup> (see **2-3-1** and **4-1-3** in this special issue). The system

reproduces CME occurrence and the propagation process of interplanetary shock waves associated with the CME through a three-dimensional numerical simulation, and determines the arrival time of these shock waves from simulated data for use in predicting space environmental disturbances caused by CME events. The system has three features, the first being that the system determines both the process of CME propagation and ambient solar wind conditions through numerical simulation. While an empirical model (described later) is used to generate CME and reproduce ambient solar wind, modeling based on simulation that solves an equation of time evolution has enabled us to obtain the whole process of shock wave propagation and capture the interaction between CME and ambient solar wind. The feature second is that, given a computing execution taking only hours to about one-fourth of a day to complete, results are made available days before the commencement of disturbances based on CME occurrence information obtained earlier, thereby making it possible to predict when CME-induced disturbances will occur. The third feature is that the entire workflow from computing through intermediate processing (i.e., visualizing the process of shock wave propagation) and retrieving results, to comparisons with observational data can be conducted via the Web,

and all activities after submission of jobs for computing appear on the Web automatically, making prior experience in supercomputer usage nonessential.

This paper provides a detailed description of the prediction system.

## 2 System configuration

Figure 1 is the system configuration. When the system receives observation information about the occurrence of a CME event from LASCO onboard the *SOHO* spacecraft, the solar wind density and velocity data at that time observed by the *ACE* satellite at the L1 point are input to determine the status of global solar wind (ambient solar wind). The LASCO-observed expansion speed data of the CME and the information about the location of that CME occurrence are also input as CME initial conditions. A job is then submitted to the supercomputer at NICT to start a numerical simulation. The way CME departs from the solar surface and shock waves form and propagate is visualized at fixed time intervals, and appears on the Web automatically. The simulation ends automatically the moment the shock waves pass the L1 point. The time at which the waves pass the L1 point then appears in a table on the Web, along with the simulated solar wind density and velocity at that time. The process up to

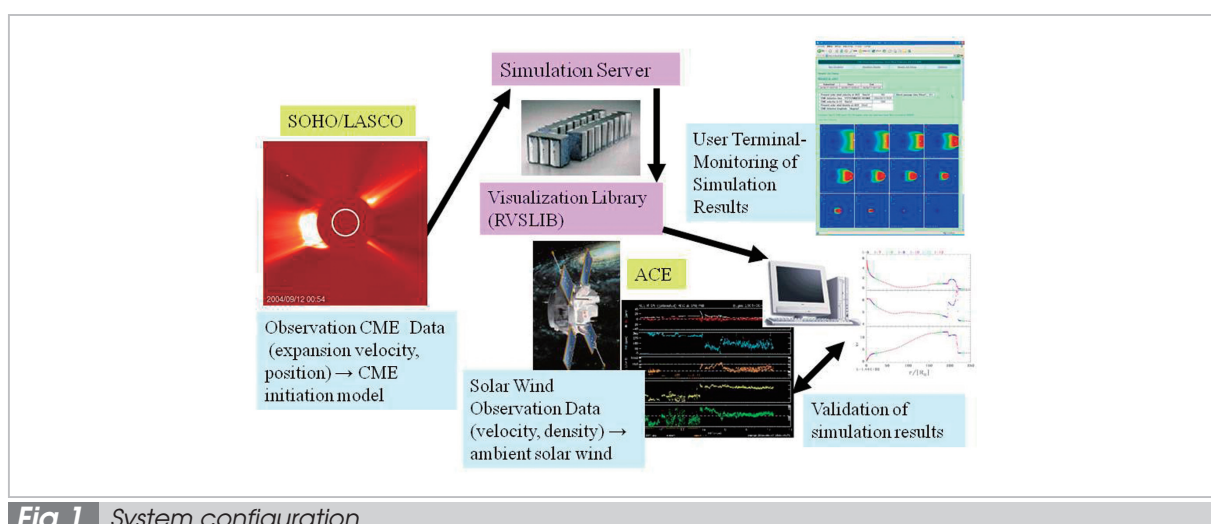


**Fig. 1** System configuration

this point takes less than one-fourth of a day from the start of computation. Because actual shock waves typically take about one day to arrive in case of very fast CME, and often several days to arrive near the earth, the simulation can be made a practical tool for forecasting. When the *ACE* satellite observes an actual shock wave arriving near the earth, the observed solar wind data are input into the table on the Web. The entire sequence of entry tasks can be performed via the Web, without needing prior experience in supercomputer usage or related knowledge. Here, the time taken by shock waves to arrive at the L1 point is determined and compared with observational data, but it should be noted that shock waves take another hour or so to reach the geomagnetosphere from the L1 point.

### 3 Simulation model

This chapter describes the simulation methodology, the ambient solar wind model, and the CME model used in this prediction model.

#### 3.1 Simulation methodology

We solve a three-dimensional hydrodynamic equation in our simulations in this system. Interplanetary magnetic fields are known to induce massive geomagnetic disturbances when facing southward. To predict the intensity of CME-induced disturbances in the geomagnetosphere, it is necessary to solve magnetohydrodynamic equations. Here, we focus on predicting the time at which CME-induced disturbances will arrive near the earth, and it is possible to estimate that time from the propagation velocity of shock waves associated with CME. As the shock waves leave the solar disk by a certain distance, their kinetic energy dominates, thereby making magnetic energy and thermal energy negligible. Assuming dipolar distributions of the solar magnetic field, if magnetic field intensity on the solar surface is 0.5 mT and CME having an expansion velocity of 800 km/s is generated at 3 Rs, and the solar

wind has a density of  $10^5 \text{ cm}^{-3}$  and temperature of 1.6 MK, then the magnetic pressure, thermal pressure and ram pressure would be  $4000 \mu \text{ Pa}$ ,  $4 \mu \text{ Pa}$  and  $50 \mu \text{ Pa}$ , respectively, with magnetic pressure being dominant near the sun (magnetic field intensity of  $19 \mu \text{ T}$  at 3 Rs). At 30 Rs apart from the sun, however, if the magnetic field intensity, solar wind density, temperature and velocity were estimated at  $19 \text{ nT}$ ,  $250 \text{ cm}^{-3}$ ,  $0.3 \text{ MK}$  and  $800 \text{ km/s}$ , respectively, the magnetic pressure, thermal pressure and ram pressure would equal  $4 \text{ nPa}$ ,  $2 \text{ nPa}$  and  $130 \text{ nPa}$ , respectively. The ram pressure is dominant at this point and this condition is always satisfied outward, suggesting that it is a good approximation to solve hydrodynamic equations for evaluation of the shock wave propagation.

The equations to solve are:

$$\frac{\partial \rho}{\partial t} + \nabla \bullet (\rho u) = 0 \quad (1)$$

$$\frac{\partial(\rho u)}{\partial t} + \nabla \bullet (\rho uu) = \rho g \quad (2)$$

$$\frac{\partial e}{\partial t} + \nabla \bullet (e + P)u = \rho g \bullet u + (\gamma - 1)Q \quad (3)$$

where,  $g$  and  $Q$  denote gravity and heating term [2], respectively, and  $\gamma$  the ratio of specific heats. These values are each stated in an equation as:

$$g = G \frac{M_s}{r^3} \mathbf{r},$$

$$Q = -\rho q_0 (T - T_0) \exp \left[ -\frac{(r - R_s)^2}{\sigma_0^2} \right] \quad (4)$$

$$\gamma = \frac{5}{3}$$

$$q_0 = 10^6 \text{ erg/g/s/K}$$

$M_s$  and  $R_s$  denote the solar mass and solar radius, respectively, and  $T_0$  is set to repro-

duce the ambient solar wind at the time of CME occurrence.

The simulation technology that we used employs the Roe-MUSCL method [4]–[6] with the third order accuracy in space, a shock-capturing scheme (a TVD method) for the flux part, and the fully threaded tree (FTT) method [7]—an adaptive mesh refinement (AMR) method—for the mesh part. The AMR method refines the mesh automatically to suit changes in physical quantities. It is appropriate for systems in which a substance is localized in matter with rarefied density and its position varies every moment, such as one in which shock waves propagate. In this simulation, the finest mesh is 1/4096 of one side of the simulation region in the vicinity of the sun, and equivalent to an equally spaced mesh of  $4096^3$ . The simulation region is a three-dimensional space—2.3 AU per side—centering on the sun.

### 3.2 Ambient solar wind model

Solar wind refers to a steady flow of plasma. As CME propagates through solar wind, the propagation velocity of CME depends on the status of this ambient solar wind, unless there is a noticeable difference in velocity between CME and the solar wind [3]. The solar corona is rather isothermal, with its ratio of specific heats close to 1. Since the mechanism of corona heating has yet to be elucidated, heating term  $Q$  is introduced in Equation (4) indicated in Section 3.1, and parameter  $T_0$  in  $Q$  is determined to match the solar wind density and velocity observed by the *ACE* satellite. Because ambient solar winds vary constantly, each time CME occurs, we read the solar wind density and velocity data at that time observed by the *ACE* satellite to find the value  $T_0$ , then we start simulation to reproduce the ambient solar wind before simulating CME propagation.

### 3.3 CME model

Various models have been proposed regarding the mechanism of CME occur-

rence, but it is not clarified yet and there is no typical CME model based on physics. Here, a CME model using parameters capable of essentially reproducing the behavior of solar wind observed by the *ACE* satellite was used based on a geometric CME model used in Reference [8]. The model can be expressed in equations as:

$$V(t, \xi) = V_{\max} A(\xi) B(t) \quad (5)$$

$$A(\xi) = \cos\left(\frac{\pi}{2} \frac{\xi}{45^\circ}\right) \quad (6)$$

$$B(t) = \begin{cases} \frac{t}{0.1h} & (0 < t < 0.1h) \\ 1 & (0.1h < t < 0.2h) \\ \frac{1.2h - t}{1.0h} & (-0.2h < t < 1.2h) \end{cases} \quad (7)$$

$A$  represents the geometry of CME, with its expansion currently being fixed. And  $B$  denotes the duration, with its value applied based on empirical rules. Because the geometry of CME and its acceleration process often vary from event to event, the application of a single model as explained above is an act of significant approximation, and should call for verification of its scope. Chapter 5 also mentions this issue.

## 4 Usage

This chapter focuses on usage of the system. Users can execute the entire workflow from executing simulation to verifying the simulation results, without exiting the Web interface. The workflow is divided into the following sequential steps:

- 1 Get input data from observation images and data, and enter the data.
- 2 Submit a simulation job.  
(Observe the propagation process)
- 3 Confirm end of the job and verify simulation results to aid in making decisions

about a forecast.

- 4 After shock waves arrive, enter actual observational data on shock waves on the result validation page.

Steps 1 to 4 deliver all visualization views and results on the Web screen automatically in parallel with the computing process, without requiring users to possess prior experience in computer simulations or using supercomputers.

Figure 2 shows the Web page for data input for simulation. Simulation input data consists of the date and time of CME occurrence (in YYYYMMDD HHMM format), its location and velocity, and the solar wind velocity and density at the L1 point when CME occurs needed to reproduce ambient solar wind. Information relevant to the CME event can be derived from LASCO images, and information relevant to solar wind can be read from real-time solar wind data delivered by the ACE satellite (see **4-1-3** in this special issue).

Figure 3 shows the web page on which the process of shock wave propagation appears. Color contours of the solar wind velocity are each shown in a 2D image as viewed from the north, with the lower-right image showing one at CME occurrence and the upper-left image showing one at the end of the computing process. The earth is located at the white point to the right of the center in each image; the sun is at the center of the

dark blue part (having solar wind velocity of 0) somewhat left of center. Use of a real-time visualization library RVSLIB (built by NEC Corporation) has allowed us to perform visualization on an SX Series supercomputer at NICT, concurrently with simulation. The simulation results are totally processed in memory, instead of being saved to storage, thus speeding up the visualization time, as well as saving I/O time and eliminating storage requirements. The simulation takes about four to seven hours to complete when executed on a single node consisting of NEC's SX-6 supercomputer. When using the present SX-8R as a single node, the computing process can be expected to finish in several hours. Since CME typically takes one to several days to arrive near the earth, the simulation model may be capable of predicting the shock waves associated with CME prior to arrival unless the CME event is an extremely fast one.

Figure 4 shows the computing result presentation page. The page holds the date and time to submitting a simulation job, starting and ending a simulation, and shows an input

LASCO:CME Initiation time(YYYYMMDD HHMM), (Initiation position), Expansion speed( $v_{exp}$ )	
ACE: Present solar wind speed( $v_{sw}$ ), (solar wind density)	
<input type="text" value="Present solar wind velocity at ACE (km/s)"/> (km/s) <input type="text" value="CME initiation time (YYYY/MM/DD HHMM)"/> (YYYYMMDD) <input type="text" value="CME velocity in C2 (km/s)"/> (km/s) <input type="text" value="Present solar wind density at ACE (/cc)"/> (/cc) <input type="text" value="CME initiation longitude (degree)"/> (degree) <input type="text" value="Comment"/> <input type="button" value="Submit"/>	

**Fig.2** Data input page

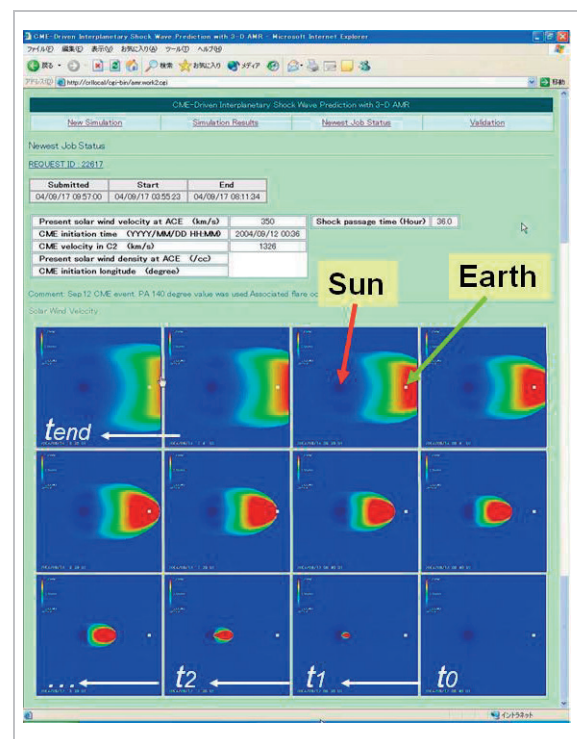


**Fig.3** Propagation of shock waves

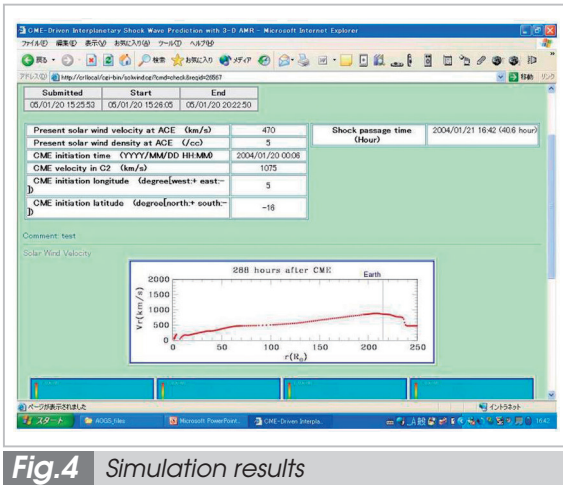


**Fig.4** Simulation results

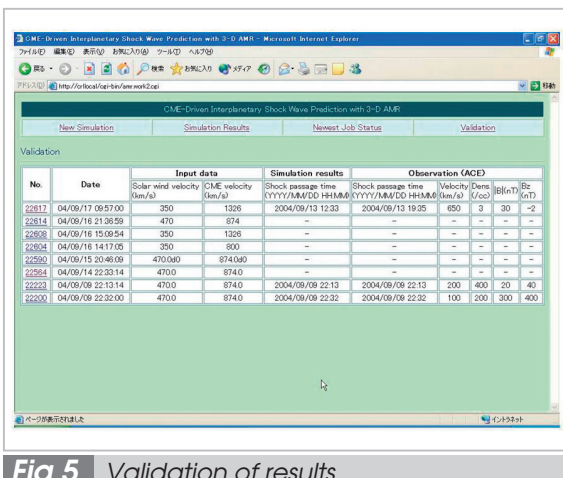


**Fig.5** Validation of results

data table and the simulated shock wave arrival time. A one-dimensional plot of solar wind velocity in the radial direction emerges with the distance between the sun and earth being taken on the axis of abscissa. This diagram is also visualized automatically and refreshed at fixed time intervals. It offers a quantitative insight into the time evolution of velocity.

Figure 5 shows the result validation page that summarizes information about previously simulated CME events in a list view. The date and time at which a shock wave actually arrived near the earth are read from observational data and entered manually. The simulation can thus be compared with observational data to verify the simulation model and, moreover, the data can be recorded and com-

piled into an event list to aid in analysis study.

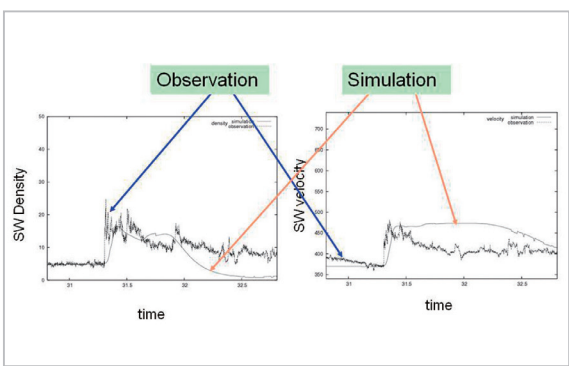
## 5 Model review

Table 1 summarizes simulated data on seven CME events versus the associated observational data [9]. Each numeral in the rightmost column indicates the percentage ratio of the difference between the simulation and actual propagation time to the actual propagation time. The positive sign denotes an instance of propagation predicted to occur earlier than observed; the negative sign denotes propagation predicted to occur later. Most instances of such prediction fell within about 20% of the observational data. The failure of simulations to match associated observational data can be attributed to either the occurrence of multiple CME events (first, fourth and fifth events) or not a remarkable difference in velocity between CME and ambient solar wind (sixth event). In the first case, one CME event had been immediately preceded by the occurrence of another CME event, whose impact on the ambient solar wind may not have been reflected. When an active region exists on the solar disk, multiple CME events occurring in succession may interact with one another. Such a situation would be hardly applicable to the present model, because it assumes a quiet solar wind blowing prior to CME occurrence. In the latter case, CME having a relatively slow velocity of 600 km/s would be intensely affected by ambient solar wind. Hence, an ambient solar wind model capable of reproducing a sector structure or current sheet position is needed. For the fourth CME event in which the simulation deviates most from the observational data, propagation was predicted to occur about 10 hours later than observed. Although this marks no small time difference, by allowing for a possible deviation of about 20% beforehand, the simulation could be made useful in terms of providing forecast information.

Figure 6 shows the time evolutions of

**Table 1** Simulated data validation table

No.	CME initiation date and time	Shock wave passage date and time (Simulation result)	Shock wave passage date and time (Observation)	Difference (ratio)
1	2001/01/20 21:54	01/23 10:06	01/23 02:31	-13%
2	2001/01/28 15:54	01/31 07:23	01/31 08:10	+1%
3	2001/08/25 16:50	08/27 19:19	08/27 22:30	+6%
4	2001/10/19 16:50	10/21 16:12	10/22 02:28	+22%
5	2001/10/25 15:26	10/28 02:42	10/28 01:59	-1%
6	2002/05/16 00:50	05/18 19:19	05/19 08:16	+19%
7	2004/01/20 00:06	01/22 01:04	01/22 02:03	+2%



**Fig.6** Comparison of simulated and observational data

solar wind density (left) and velocity (right) of a given CME event on the *ACE* satellite orbit. Time is taken on the axis of abscissa, and noisy curves represent observational data whereas smooth curves represent simulated data. Both density and velocity match with good accuracy at the front of shock waves regarding both time and physical quantities, but not so accurately at the rear. This is because the rear part of shock waves is a structural component of CME (such as a flux rope) and not taken into account into the geometric CME model as described in Section 3.3. In fact, this component had been left out of the model's scope at the beginning. The rear part of a shock wave is not an object of direct prediction, but if it involves a flux rope, it often occurs in major geomagnetic disturbances. The development of a more accurate CME model at remains a future challenge.

## 6 Conclusions

We have developed a system for predict-

ing the arrival of shock waves associated with CME near the earth, based on a three-dimensional numerical simulation. The simulation technology that we used employs the Roe-MUSCL method, one of the TVD methods capable of handling shock waves with stability, as a differential scheme in a flux part, and an adaptive mesh refinement (AMR) method that makes the accuracy variable from moment to moment to meet changes in physical quantities for the mesh. The system is characterized by its ability to reproduce a solar wind blowing prior to CME occurrence and follows the propagation of CME through solar wind, thereby involving the interaction between ambient solar wind and CME. Visualization processing is automated and the entire workflow from data input through starting a simulation and validating simulation results is carried out via the Web interface, without requiring users to possess prior experience in numerical simulations or using supercomputers. Simulation is also expected to only take several hours on the available NICT supercomputer to complete, fully ahead of the actual arrival of shock waves associated with an actual CME event, thereby making the system a practical tool for forecasting.

Phenomena beyond the scope of this system, such as interactions among multiple CME events, tend to occur frequently as the solar activity increases. The task of developing a model of the shock wave propagation process for applicability under such conditions demanding caution for the space environment remains a key challenge for the future.

The use of a more realistic solar wind model and CME model should be worth considering. As for solar winds, some allowance might be made for the magnetic field, including such solar wind structures as the sector structure and current sheet position. Our ongoing probe into the process of shock wave propagation through solar wind simulated in a current sheet has demonstrated that the time at which shock waves arrive varied

drastically depending on their positional relation with the current sheet, suggesting that solar wind structures made more precise could be a key factor in determining propagation.

tion [10]. The CME model might also be made physical. Research on the mechanism of CME occurrence is now underway, with further advances being anticipated.

## References

- 1 M. Den, T. Tanaka, S. Fujita, T. Obara, H. Shimazu, H. Amo, Y. Hayashi, E. Nakano, Y. Seo, K. Suehiro, H. Takahara, and T. Takei, "Real-time Earth magnetosphere simulator with three-dimensional magneto-hydrodynamic code," *Space Weather*, Vol. 4, S06004, doi: 10.1029/2004SW000100, 2006.
- 2 W. B. Manchester, T. I. Gombosi, I. Roussev, A. Ridley, D. I. De Zeeuw, I. V. Sokolov, K. G. Powell, and G. Toth, "Modeling a space weather event from the Sun to the Earth: CME generation and interplanetary propagation," *J. Geophys. Res.*, Vol. 109, pA02107, 2004.
- 3 M. Tokumaru, M. Kojima, K. Fujiki, and A. Yokobe, "Three-dimensional propagation of interplanetary disturbances detected with radio scintillation measurements at 327 MHz," *J. Geophys. Res.*, Vol. 105, No. A5, pp. 10,435–10,453, 2000.
- 4 P. L. Roe, "Approximate Riemann solvers, parameter vectors, and difference schemes," *J. Comp. Phys.*, Vol. 43, pp. 357–372, 1981.
- 5 B. van Leer, "Towards the ultimate conservative difference scheme, IV. a new approach to numerical convection," *J. Comp. Phys.*, Vol. 23, pp. 276–299, 1977.
- 6 B. van Leer, "Towards the ultimate conservative difference scheme, V. a second-order sequel to Godunov's method," *J. Comp. Phys.*, Vol. 32, pp. 101–136, 1979.
- 7 A. M. Khokhlov, "Fully threaded tree algorithms for adaptive refinement fluid dynamics simulations," *J. Comp. Phys.*, Vol. 143, pp. 519–543, 1998.
- 8 D. Odstrcil and V. J. Pizzo, "Three-dimensional propagation of coronal mass ejections (CMEs) in a structured solar wind flow 2. CME launched adjacent to the streamer belt," *J. Geophys. Res.*, Vol. 104, pp. 483–492, 1999.
- 9 T. Ogawa, M. Den, T. Tanaka, and K. Yamashita, "Simulation of Interplanetary Shock Wave Caused by CME on August 25 2001," *Adv. in Geosciences*, No. 2, p. 6571, 2006.
- 10 T. Ogawa, M. Den, T. Tanaka, K. Sugihara, T. Takei, H. Amo, S. Watari, and K. Yamashita, "Testing model for prediction system of 1-AU arrival time of CME-associated interplanetary shocks," in paper number PSW1-0022-08 presented in COSPAR 2008.



**DEN Mitsue, Ph.D.**  
Senior Researcher, Space Environment Group, Applied Electromagnetic Research Center  
Astrophysics



**TANAKA Takashi, Dr. Sci.**  
Professor, Graduated School of Sciences, Kyushu University  
Magnetospheric Compound System Physics



**WATARI Shinichi, Dr. Sci.**  
Research Manager, Space Environment Group, Applied Electromagnetic Research Center  
Solar-Terrestrial Physics, Space Weather

**AMO Hiroyoshi, Dr. Sci.**  
NEC Corporation  
Information Engineering

**SUGIHARA Kouta, Dr. Sci.**  
NEC Corporation  
Information Engineering

**TAKEI Toshifumi, Dr. Sci.**  
NEC Corporation  
Information Engineering